Iranian Journal of Organic Chemistry Vol. 8, No. 2 (2016) 1777-1787

Structural and energetically study on nitro and amino derivatives of 1,2,3,5-tetrazine

Mehdi Nabati[a]*, Mahsa Hojjati[b]

[a]*Chemistry Department, Faculty of Science, Azarbaijan Shahid Madani University, Tabriz, Iran*
[b]*Inorganic Research Laboratory, Faculty of Chemistry, Shahrood University of Technology, Shahrood, Iran*

Received: February 2016; Revised: March 2016; Accepted: April 2016

Abstract: Although many tetrazine based compounds have been synthesized and studied theoretically, the chemistry of molecules based on 1,2,3,5-tetrazine are little known. In the present study, the nitro and amino derivatives of 1,2,3,5-tetrazine were designed and investigated to get molecular geometries and electronic structures at ab-initio and density functional theory (DFT, B3LYP) at the levels of 6-31G(d,p), 6-31+G(d,p), 6-311G(d,p), 6-311+G(d,p) and cc-pvDZ. Some important properties such as bond dissociation enthalpy, density, frontier orbital energy, thermodynamic parameters, nucleus-independent chemical shifts (NICSs), and heat of formation and detonation parameters were then calculated. Also, IR and NMR spectra of the structures were simulated. The volumes of the structures computed to get the densities of the molecules. The heats of formations (HOFs) were estimated via isodesmic reactions. All calculations carried out in gas phase at temperature 298 K and pressure 1 atm. It deduced that the introduction of nitro group can improve the detonation properties of the structures. The simulation results revealed that these compounds exhibit excellent performance; and the all structures are viable candidate of high energy density materials (HEDMs). Comparing the detonation properties of molecules with standards (RDX and HMX) shows 4,6-dinitro-1,2,3,5-tetrazine can be an explosive.

Keywords: Nitrogen-rich compounds, Tetrazine, Bond dissociation energy, Heat of formation, Detonation properties.

Introduction

Research in the field of energetically compounds frequently emphasizes the preparation of organic energetic materials containing the nitro-groups. The nitro-groups are responsible for oxidation of the hydrogen and carbon atoms. The water and carbon dioxide are the ultimate products from the oxidation procedure of the energetic materials. All products (H_2O, CO, CO_2, H_2 and C) have very negative heats of formation [1]. In spite of this, there are very few examples, even for highly nitrated molecules, which possess enough oxygen to completely oxidize the carbon in the backbone to carbon dioxide.

As a consequence, the solid carbon and unoxidised organic segments of energetic materials prepare a large quantity of residue and smoke during detonation or combustion procedures [2, 3]. The strong exothermic reactivity of high energy density materials (HEDMs) cause them desirable for both military and commercial applications. The identification and characterization of these molecules are very difficult. Approaches to this, include conventional chemical and analytical methods. However, the conventional methods are time consuming and are not eco-friendly, because they need large quantity of reagents, solvents and glass wares. Two important parameters in designing better energetic molecules are the detonation decomposition products and oxygen balance [4, 5]. The tetrazine ring system is the six-membered heterocyclic organic compound with

*Corresponding author. Tel: (+98) 1723389112, Fax: (+98) 1723389101, E-mail: mnabati@ymail.com

four nitrogen atoms and two carbon atoms. The 1,2,3,5-tetrazine and its' derivatives weren't synthesized nowadays. Computational chemistry is used in different ways [6]. The main technique is a molecular system modeling prior to producing that compound in the laboratory. This technique is a very good method because preparing a molecule could require months of labor and various reagents, and produces toxic waste [7]. The complete consideration of a compound is the second use of theoretical chemistry [8]. Some properties and performances of a compound can be obtained theoretically more easily than by experimental methods [9]. In recent years, the density functional theory (DFT) has become very popular between all of computational chemistry methods. This is justified based on the pragmatic observation that it is less computationally intensive than other methods with similar accuracy. This theory has been developed more recently than other ab-initio methods [10, 11]. In this paper, stabilities of six structures as potential candidates for high energy density materials (HEDMs) have been investigated theoretically by using quantum chemical treatment. Geometric features, electronic structures of these sym-tetrazine derivatives have been systematically studied using ab initio and density functional theory (DFT, B3LYP) at the level of 6-31G(d,p), 6-31+G(d,p), 6-311G(d,p), 6-311+G(d,p), cc-pvDZ. Moreover, these molecules properties were investigated at B3LYP/6-311G(d,p) level.

Results and discussion

The geometries of interested molecules:

The studied six molecules are 1,2,3,5-tetrazine (A), 4-amino-1,2,3,5-tetrazine (B), 4,6-diamino-1,2,3,5-tetrazine (C), 4-nitro-1,2,3,5-tetrazine (D), 4,6-dinitro-1,2,3,5-tetrazine (E) and 4-amino-6-nitro-1,2,3,5-tetrazine (F). The molecular frameworks of six title compounds are displayed in Figure **1**. The chemical structures and atomic numbering of the compounds are showed in Figure **2**. The geometric structures of the molecules with electron charge of the elements of each compound are showed in Figure **3**. The dipole moments of the molecules are listed in Table **1**. As seen from the table, the μ order is F>C>B>D>A>E for the structures at B3LYP/6-311G(d,p) level of theory.

Bond lengths, Bond Angles and Dihedral Angles:

The bond lengths data of the molecules have been given in Table **2**. It is obtained that all the N-N and C-N bonds in the tetrazine rings are changed by introducing of amino and nitro groups. From data, it is observed that the C-NH_2 bond is shorter than the C-NO_2 bond. Electrostatic potential maps, also known as electrostatic potential energy maps, or molecular electrical potential surfaces, illustrate the charge distributions of molecules three dimensionally. These maps allow us to visualize variably charged regions of a molecule. Knowledge of the charge distributions can be used to determine how molecules interact with one another [18]. Electrostatic potential maps are very useful three dimensional diagrams of molecules. They enable us to visualize the charge distributions of molecules and charge related properties of molecules. They also allow us to visualize the size and shape of molecules. In organic chemistry, electrostatic potential maps are invaluable in predicting the behavior of complex molecules [19]. The three-dimensional electrostatic potential maps of the structures are shown in Figure **4**. The red loops and the blue loops indicate negative and positive charge development for a particular system respectively. As can be seen from the figures the negative charge is located on the nitrogen elements of the tetrazine ring and the nitro groups as expected due to the electron withdrawing character of them and positive charge is located on the amino groups as expected due to the electron donating character of amino groups in the structure. However, charge development on nitrogen elements of rings decreases with increasing number of nitro groups in the structure and also it increases with increasing number of amino groups in the structure.

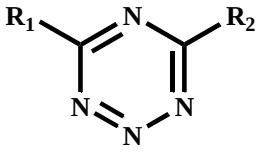

A: R_1=R_2=H **D: R_1=NO_2 , R_2=H**
B: R_1=NH_2 , R_2=H **E: R_1=R_2=NO_2**
C: R_1=R_2=NH_2 **F: R_1=NO_2 , R_2=NH_2**

Figure 1: Molecular frameworks of studied compounds.

The bond angles data of the molecules have been given in Tables **3** and **4**. It is observed that the C-NH_2 bond length is shorter than C-NO_2 bond length in the F structure as expected due to the electron donating and electron withdrawing characters of the groups. Also, it is obtained that the nitro and amino group decrease H-N-H and O-N-O angles in the F structure respectively. The dihedral angles of structures show us that all of the structures aren't planar.

Table 1: Dipole moments of the structures.

Structures	μ_X (Debye)	μ_Y (Debye)	μ_Z (Debye)	μ_{Tot} (Debye)
A	0.0001	2.6664	0.0000	2.6664
B	4.0060	2.2420	0.0031	4.5907
C	-0.0004	-4.8694	0.0108	4.8694
D	2.0754	2.4088	0.0006	3.1796
E	-0.0001	0.1953	-0.0001	0.1953
F	-5.2834	-3.5700	0.5906	6.4037

Table 2: Bond lengths of structures calculated at B3LYP/6-311G(d,p) level of theory.

Bonds (Aº)	A	B	C	D	E	F
N1-C2	1.329	1.340	1.333	1.315	1.317	1.308
C2-N3	1.338	1.362	1.361	1.323	1.326	1.320
N3-N4	1.323	1.306	1.312	1.328	1.324	1.340
N4-N5	1.323	1.330	1.312	1.319	1.323	1.298
N5-C6	1.338	1.339	1.361	1.339	1.326	1.366
C6-N1	1.329	1.323	1.334	1.331	1.318	1.342
C2-H7	1.085	-	-	-	-	-
C6-H8	1.085	1.087	-	1.084	-	-
C2-N7	-	1.343	1.346	1.489	1.487	1.504
C6-N8	-	-	1.346	-	1.487	1.337
N7-H9	-	1.006	1.005	-	-	-
N7-H10	-	1.006	1.006	-	-	-
N8-H11	-	-	1.005	-	-	1.007
N8-H12	-	-	1.005	-	-	1.006
N7-O9	-	-	-	1.215	1.214	1.216
N7-O10	-	-	-	1.215	1.214	1.214
N8-O11	-	-	-	-	1.214	-
N8-O12	-	-	-	-	1.213	-

Table 3: Bond angles of the structures calculated at B3LYP/6-311G(d,p) level of theory.

Bond angles (degree)	A	B	C	D	E	F
N1-C2-N3	125.494	124.458	125.350	128.252	127.765	129.384
C2-N3-N4	117.967	118.062	117.312	116.420	116.918	115.454
N3-N4-N5	120.456	121.327	122.110	120.399	120.360	121.263
N4-N5-C6	117.935	117.069	117.296	118.423	116.929	118.572
N5-C6-N1	125.503	126.564	125.330	125.063	127.750	123.741
C6-N1-C2	112.644	112.521	112.602	111.442	110.280	111.501
N1-C2-H7	118.351	-	-	-	-	-
N1-C2-N7	-	119.066	118.736	116.509	116.697	115.545
N3-C2-H7	116.155	-	-	-	-	-
N3-C2-N7	-	116.476	115.915	115.238	115.538	115.070
N5-C6-H8	116.144	115.858	-	116.635	-	-
N5-C6-N8	-	-	115.927	-	115.538	116.884
N1-C6-H8	118.353	117.578	-	118.302	-	-
N1-C6-N8	-	-	118.743	-	116.712	119.373
C2-N7-H9	-	119.615	119.828	-	-	-
C2-N7-H10	-	119.222	118.895	-	-	-
H9-N7-H10	-	121.163	121.271	-	-	-
C2-N7-O9	-	-	-	115.864	115.610	116.016
C2-N7-O10	-	-	-	115.833	115.572	116.219
O9-N7-O10	-	-	-	128.302	128.818	127.765
C6-N8-O11	-	-	-	-	115.555	-
C6-N8-O12	-	-	-	-	115.647	-
O11-N8-O12	-	-	-	-	128.798	-
C6-N8-H11	-	-	119.774	-	-	119.822
C6-N8-H12	-	-	118.896	-	-	119.210
H11-N8-H12	-	-	121.330	-	-	120.928

Table 4: Dihedral angles of the structures calculated at B3LYP/6-311G(d,p) level of theory.

Dihedral angles (degree)	A	B	C	D	E	F
N1-C2-N7-H9	-	1.548	-0.506	-	-	-
N1-C2-N7-H10	-	179.886	-179.658	-	-	-
N3-C2-N7-H9	-	-179.926	179.601	-	-	-
N3-C2-N7-H10	-	-0.034	0.450	-	-	-
N5-C6-N8-H11	-	-	179.899	-	-	178.360
N5-C6-N8-H12	-	-	0.105	-	-	0.632
N1-C6-N8-H11	-	-	-0.127	-	-	-1.136
N1-C6-N8-H12	-	-	-179.922	-	-	-178.863
N1-C2-N7-O9	-	-	-	-89.968	90.097	48.531
N1-C2-N7-O10	-	-	-	89.886	-89.957	-131.308
N3-C2-N7-O9	-	-	-	90.022	-89.942	-131.088
N3-C2-N7-O10	-	-	-	-90.124	90.005	49.074
N5-C6-N8-O11	-	-	-	-	90.125	-
N5-C6-N8-O12	-	-	-	-	-89.950	-
N1-C6-N8-O11	-	-	-	-	-89.962	-
N1-C6-N8-O12	-	-	-	-	89.963	-
C6-N1-C2-N7	-	-180.000	-179.902	180.000	-179.965	178.950
C2-N1-C6-N8	-	-	-179.983	-	180.000	-177.661
N4-N3-C2-N7	-	180.000	179.943	179.978	180.000	178.488
N4-N5-C6-N8	-	-	179.954	-	179.964	178.820
N1-C2-N3-N4	7.146	0.057	0.047	-0.037	-0.041	-1.067
C2-N3-N4-N5	-6.174	-5.275	-0.072	0.067	-1.277	2.459
N3-N4-N5-C6	-1.216	-0.020	0.058	-0.036	-2.800	-1.196
N4-N5-C6-N1	-4.080	5.792	-6.203	-3.171	0.048	-1.708
N5-C6-N1-C2	5.946	5.631	6.487	0.035	-0.087	2.879
C6-N1-C2-N3	-1.376	-0.063	-2.874	-1.174	0.084	-1.697

Nucleus Independent Chemical Shifts (NICS):

Aromaticity continues to be an actively investigated area of chemistry. In 1996, Schleyer has proposed the new method as an aromaticity/antiaromaticity criterion [20].

Table 5: NICS values for the structures calculated at B3LYP/6-311G(d,p) level of theory.

Structures	NICS
A	-2.032
B	-0.423
C	-0.265
D	-4.348
E	-5.257
F	-2.204

The nucleus-independent chemical shift (NICS) is a computational method that calculates the absolute magnetic shieldings at the center of the ring taken with reversed sign. In this method negative NICS values indicate aromaticity and positive values antiaromaticity. In this study, NICS values of the tetrazine derivatives have been calculated by the application of density functional theory using the standard 6-311G(d,p) basis set (Table **5**). Nitro derivatives of tetrazine (D, E) have been found to be aromatic but other structures (A, B, C and F) have been found to be non-aromatic. The nitrogen atoms in the rings are higher electronegativity than carbon atoms and for this reason, the electrons located on the nitrogen atoms. In the D and E structures, the electrons have been pulled into the rings by the attachment of very strongly withdrawing nitro groups.

Infrared spectra:

The IR spectrum is one basic property of a compound, and also an effective measure to identify structures. Here, vibrational frequencies were calculated by using B3LYP/6-311G(d,p) level. Figure **5** provides structures' IR spectra.

Harmonic frequencies (cm^{-1}), IR intensities (KM/Mole)

A: 297.99 (16.34), 677.52 (6.51), 732.87 (8.88), 809.07 (11.21), 912.91 (27.29), 956.86 (0.03), 1014.48 (0.73), 1140.75 (5.31), 1183.05 (6.59), 1197.75 (2.51), 1392.81 (38.57), 1409.84 (26.26), 1518.99 (97.27), 1578.20 (27.05), 3176.68 (14.71), 3179.83 (2.32).

B: 145.66 (0.0004), 248.20 (213.34), 343.52 (15.67), 396.04 (9.33), 569.76 (2.03), 577.32 (1.74), 603.87 (0.95), 712.92 (3.40), 849.61 (20.32), 906.93 (0.74), 963.44 (75.02), 1000.44 (0.81), 1040.76 (3.51), 1062.59 (16.75), 1147.84 (28.73), 1329.45 (5.49), 1376.20 (34.51), 1466.23 (23.89), 1546.98 (152.14), 1573.13 (114.58), 1654.22 (491.29), 3167.21 (16.12), 3608.02 (110.24), 3742.59 (73.31).

C: 146.79 (0.03), 154.11 (240.51), 174.56 (0.01), 195.21 (184.32), 332.32 (9.56), 453.63 (4.68), 474.75

(17.53), 573.27 (0.003), 575.06 (1.02), 602.33 (1.27), 607.96 (0.3), 745.03 (0.0001), 827.97 (0.002), 843.95 (28.19), 980.48 (20.77), 1007.77 (14.49), 1038.28 (0.51), 1092.39 (149.75), 1172.21 (1.71), 1289.31 (2.78), 1415.32 (50.31), 1511.87 (50.57), 1558.46 (107.27), 1562.93 (335.37), 1633.24 (900.11), 1668.69 (112.99), 3613.60 (174.54), 3615.54 (25.74), 3750.58 (31.66), 3750.92 (100.95).

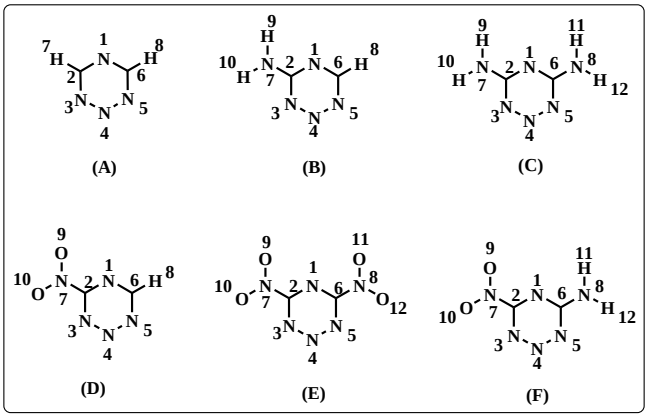

Figure 2: The chemical structures and their atomic numbering.

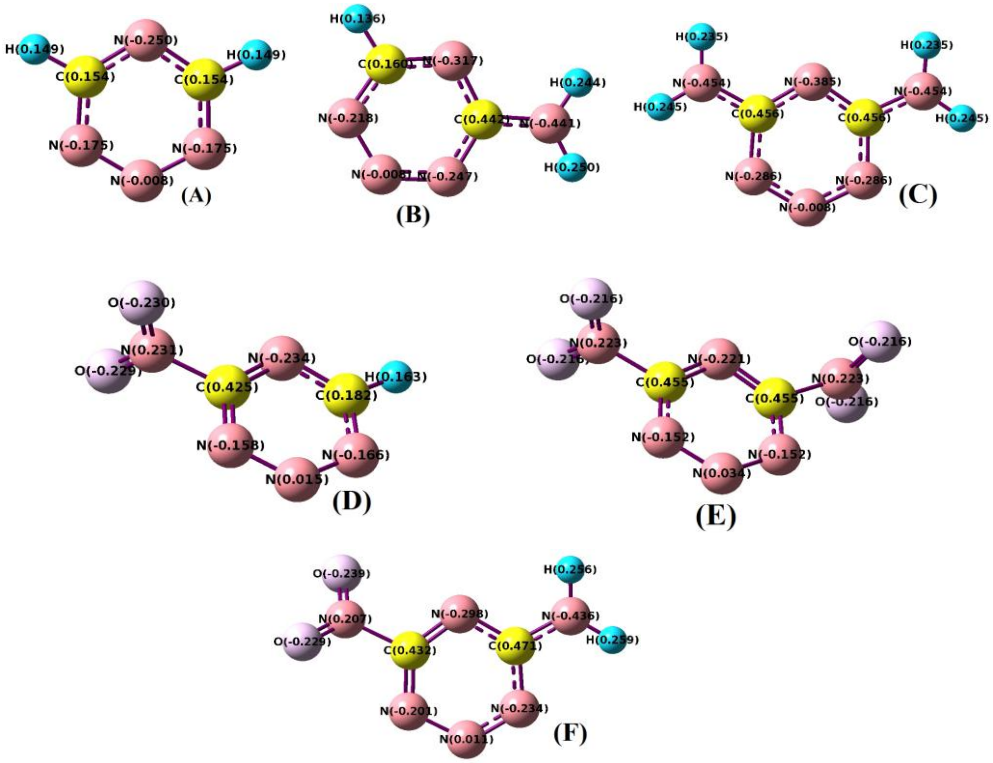

Figure 3: The geometric structures of the molecules.

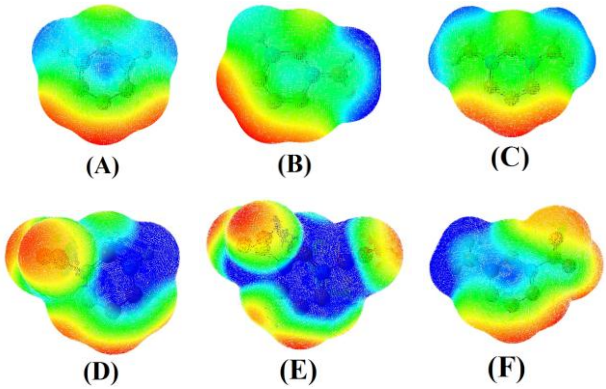

Figure 4: The 3-D electrostatic potential maps of the structures.

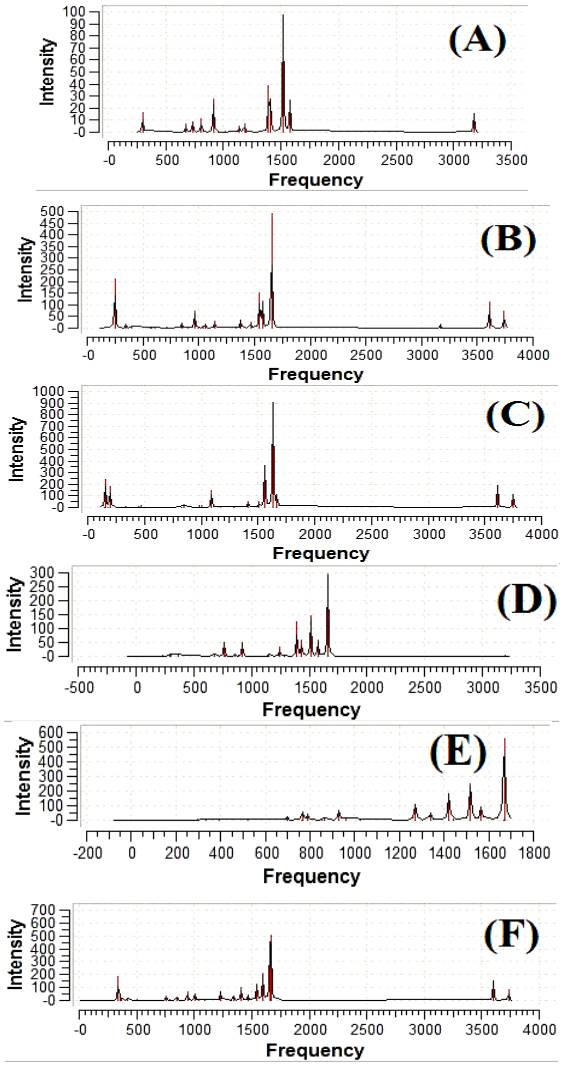

Figure 5: The IR spectra of structures.

D: 46.92 (0.55), 112.28 (1.34), 227.97 (3.88), 296.70 (6.08), 300.87 (7.08), 366.54 (3.54), 617.91 (0.03), 681.70 (10.14), 764.25 (51.22), 772.17 (3.21), 854.92 (8.07), 888.45 (2.03), 921.61 (48.00), 997.12 (1.40), 1021.22 (0.47), 1149.38 (6.42), 1247.94 (34.83), 1285.38 (3.73), 1394.30 (123.14), 1436.10 (57.06), 1513.67 (147.80), 1575.95 (56.94), 1661.14 (293.99), 3195.70 (2.40).

E: 44.94 (0.02), 95.77 (3.92), 141.97 (3.72), 278.83 (1.56), 298.82 (7.50), 332.31 (1.95), 395.94 (6.90), 520.39 (2.69), 698.02 (20.83), 763.08 (0.0003), 765.88 (60.42), 790.07 (35.70), 851.20 (5.21), 863.72 (12.36), 928.67 (65.45), 958.53 (10.23), 1023.81 (0.20), 1217.42 (1.01), 1271.22 (110.49), 1340.02 (51.22), 1421.59 (185.81), 1439.28 (10.91), 1518.10 (249.19), 1565.69 (90.76), 1665.49 (0.0003), 1668.99 (559.13).

F: 37.13 (1.40), 127.32 (1.06), 156.46 (1.55), 204.48 (3.08), 340.39 (182.97), 352.38 (18.41), 367.24 (16.20), 420.20 (14.18), 503.34 (10.40), 586.26 (0.82), 599.76 (1.24), 691.72 (3.62), 753.35 (31.31), 792.19 (10.58), 851.72 (14.61), 855.48 (21.93), 940.72 (66.87), 1006.41 (53.48), 1039.86 (2.97), 1088.38 (8.62), 1228.92 (69.26), 1342.36 (34.96), 1409.61 (98.64), 1469.61 (44.37), 1545.31 (130.49), 1597.47 (207.37), 1658.71 (297.01), 1666.30 (506.08), 3600.78 (148.43), 3733.14 (86.03).

NMR study:

The NMR analysis is an important property of a compound, and also an effective measure to identify structures. Here, the nucleus shielding (ppm) for the structures was calculated by using B3LYP/6-311G(d,p) level.

A: -321.516 (N4), -182.749 (N3), -182.701 (N5), -29.285 (N1), 21.809 (C2), 21.810 (C6), 22.459 (H7), 22.460 (H8).

B: -314.291 (N4),-137.438 (N5), -136.963 (N3), 21.786 (C2), 22.749 (N1), 23.313 (H8), 23.521 (C6), 27.151 (H10), 27.722 (H9), 171.226 (N7).

C: -303.850 (N4), -99.391 (N3), -99.346 (N5), 22.688 (C2), 22.690 (C6), 27.463 (H10), 27.464 (H12), 28.126

(H9), 28.127 (H11), 70.908 (N1), 173.963 (N7), 173.965 (N8).
D: -386.670 (O9), -386.669 (O10), -337.571 (N4), -192.058 (N5), -153.912 (N3), -140.866 (N7), -3.082 (N1), 16.992 (C2), 20.455 (C6), 22.328 (H8).
E: -392.064 (O10, O12), -392.062 (O9), -392.060 (O11), -353.908 (N4), -162.590 (N3), -162.583 (N5), -135.458 (N7, N8), 18.443 (C2), 18.444 (C6), 20.751 (N1).
F: -365.058 (O9), -359.535 (O10), -326.205 (N4), -151.453 (N5), -140.861 (N7), -111.904 (N3), 16.523 (C2), 19.607 (C6), 26.579 (H11), 27.237 (H12), 45.132 (N1), 165.578 (N8).

Energies of structures:

Tables **6** and **7** show the calculated total energies of the structures at spin- restricted Hartree-Fock (RHF) level and density functional theory (DFT, B_3LYP) at the 6-31G(d,p), 6-31+G(d,p), 6-311G(d,p), 6-311+G(d,p), cc-pvDZ basis sets, respectively. Total energies are corrected for zero-point vibrational energy (ZPVE). As seen from the tables, the stability order is E>F>D>C>B>A for the structures at these performed theoretical levels.

Table 6: Calculated total energies (in a.u.) for the structures at spin-restricted Hartree-Fock (RHF) method with different basis sets.

Structures	HF/6-31G(d,p)	HF/6-31+G(d,p)	HF/6-311G(d,p)	HF/6-311+G(d,p)	HF/cc-pvDZ
A	-294.554408	-294.562172	-294.615958	-294.621503	-294.577819
B	-349.597391	-349.607742	-349.671816	-349.679301	-349.623094
C	-404.641180	-404.654079	-404.728617	-404.737889	-404.669096
D	-497.995932	-498.010926	-498.112019	-498.123176	-498.040734
E	-701.429764	-701.452091	-701.600430	-701.617179	-701.496194
F	-553.043276	-553.060232	-553.172268	-553.184873	-553.090457

The total energies are corrected for ZPVE.

Table 7: Calculated total energies (in a.u.) for the structures at B3LYP method with different basis sets.

Structures	B3LYP/6-31G(d,p)	B3LYP/6-31+G(d,p)	B3LYP/6-311G(d,p)	B3LYP/6-311+G(d,p)	B3LYP/cc-pvDZ
A	-296.283542	-296.295614	-296.350729	-296.358369	-296.301642
B	-351.651131	-351.667719	-351.734071	-351.744364	-351.670776
C	-407.017030	-407.038296	-407.115752	-407.128829	-407.038318
D	-500.760389	-500.783313	-500.885879	-500.901182	-500.800350
E	-705.232598	-705.265851	-705.416298	-705.438766	-705.296285
F	-556.132539	-556.158853	-556.273417	-556.290724	-556.173970

The total energies are corrected for ZPVE.

Bond Dissociation Energies (BDE):

Bond dissociations investigation is essential and basic property for understanding the decomposition process of the High energy materials, since they are directly relevant to the stability and sensitivity of the high energy materials [21]. The energy required for bond hemolysis at 298.15 K temperature and 1 atmosphere pressure corresponds to the energy of reaction A-B → A^o + B^o, which is the bond dissociation energy of the compound A-B by definition. Therefore, the bond dissociation energy can be given in terms of following equation:

$$BDE_{(A-B)} = E_{(A^o)} + E_{(B^o)} - E_{(A-B)}$$

Where A-B corresponds for the structures, A^o and B^o stand for the corresponding product radicals after the bond dissociation, $BDE_{(A-B)}$ is the bond dissociation energy of bond A-B. The bond dissociation energy with ZPE correction can be calculated by following equation:

$$BDE_{(A-B)ZPE} = BDE_{(A-B)} + \Delta ZPE$$

The bond dissociation energies were calculated at the B3LYP/6-311G(d,p) level. Table **8** shows calculated total energies of tetrazine derivatives, fragments, NO_2 and NH_2 at the equilibrium geometries and resulting BDEs at the level of theory. As seen from the table, the relative stability order of these structures may be in the order: F(6)>B>C(4)=C(6)>F(4)>D>E(4)=E(6). It can be deduced that the BDEs for these molecules are highly substitution dependent. According to the Chung suggestion [22], the bond dissociation energy more than 20 kcal/mol corresponds for a compound to be considered as a viable candidate of high energy density

material (HEDM). Therefore, we can conclude that the all molecules are viable candidate of HEDMs.

Table 8: Calculated total energies of the structures, fragments, NH_2 and NO_2 at the equilibrium geometries and resulting bond dissociation energies (BDE).

Structures	Formula	Parent energy (hartrees)	Fragment energy (hartrees)	NO_2 energy (hartrees)	NH_2 energy (hartrees)	BDE (kcal/mol)
B	$C_2H_3N_5$	-351.73407	-295.68296	-205.12390	-55.87623	109.739
C(4)	$C_2H_4N_6$	-407.11575	-351.06769	-205.12390	-55.87623	107.825
C(6)	$C_2H_4N_6$	-407.11575	-351.06769	-205.12390	-55.87623	107.825
D	$C_2HN_5O_2$	-500.88588	-295.68296	-205.12390	-55.87623	49.586
E(4)	$C_2N_6O_4$	-705.41630	-500.21435	-205.12390	-55.87623	48.978
E(6)	$C_2N_6O_4$	-705.41630	-500.21435	-205.12390	-55.87623	48.978
F(4)	$C_2H_2N_6O_2$	-556.27342	-351.06769	-205.12390	-55.87623	51.349
F(6)	$C_2H_2N_6O_2$	-556.27342	-500.21435	-205.12390	-55.87623	114.734

Key to the notation: B(L) stands for the radical obtained from B structure by removing the functional group at position L.

Table 9: The HOMO and LUMO energies of the structures calculated at B3LYP/6-311G(d,p) level of theory.

Structures	MOs number	HOMO orbital	HOMO (a.u.)	LUMO orbital	LUMO (a.u.)	Δε (a.u.)
A	120	21 (A)	-0.27062	22 (A)	-0.11025	0.16037
B	144	25 (A)	-0.25140	26 (A)	-0.08506	0.16634
C	168	29 (A)	-0.23527	30 (A)	-0.05797	0.17730
D	168	32 (A)	-0.30243	33 (A)	-0.14130	0.16113
E	216	43 (A)	-0.33009	44 (A)	-0.16771	0.16238
F	192	36 (A)	-0.28247	37 (A)	-0.12158	0.16089

$\Delta\varepsilon = \varepsilon_{LUMO} - \varepsilon_{HOMO}$

Table 10: HOFs, predicted densities and detonation properties of the molecules.

Structures	OB_{100}	HOF (kJ/mol)	Q (kJ/g)	V (cm^3/mol)	ρ (g/cm^3)	D (km/s)	P (GPa)
A	-97.53	237.942	693.276	57.973	1.415	5.901	13.206
B	-90.69	422.079	1039.552	70.037	1.386	6.743	16.992
C	-85.68	602.554	1285.236	65.712	1.705	8.416	30.394
D	-31.49	243.039	1240.215	80.369	1.580	7.352	22.099
E	0.00	217.176	1395.394	82.707	2.080	9.441	42.931
F	-33.80	423.197	1450.242	85.518	1.661	8.030	27.224

*Average valu from 100 single-point volume calculations at the B3LYP/6-311G(d,p) level.
Q: Heat of explosion, V: Volume of explosion, D: Velocity of detonation, P: Pressure of explosion.

The frontier molecular orbital energies:

Table **9** shows the HOMO and LUMO energies (ε) of the molecules computed at B3LYP/6-311G(d,p) level of theory. The frontier orbitals energies increase by increasing amino substituent and decrease by increasing the number of nitro substituent on the 1,2,3,5-tetrazine ring. These are general trends of electron withdrawing substituents which lower the frontier orbitals energy levels and electron donating substituents which higher the frontier orbitals energy levels. The order of energy gap values, that is the difference between the LUMO and HOMO energy levels, is C>B>E>D>F>A at the B3LYP/6-311G(d,p) level of theory. Figures **6** and **7** provide the frontier orbitals map.

The heats of formation (HOF) values were calculated at B3LYP/6-311G(d,p) level and listed in the Table **10**. In this study, isodesmic reaction method is employed. In isodesmic reaction, the numbers of bonds and bond types are preserved on both sides of the reaction [23]. The accuracy of HOF obtained computationally is conditioned by the reliability of HOF of the reference compounds. The isodesmic reactions for HOF calculation are showed in Scheme **1**.

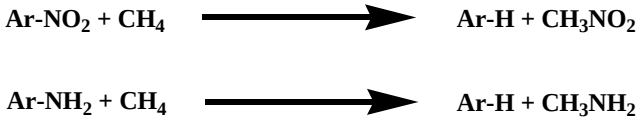

Scheme 1: The isodesmic reactions for HOF calculations.

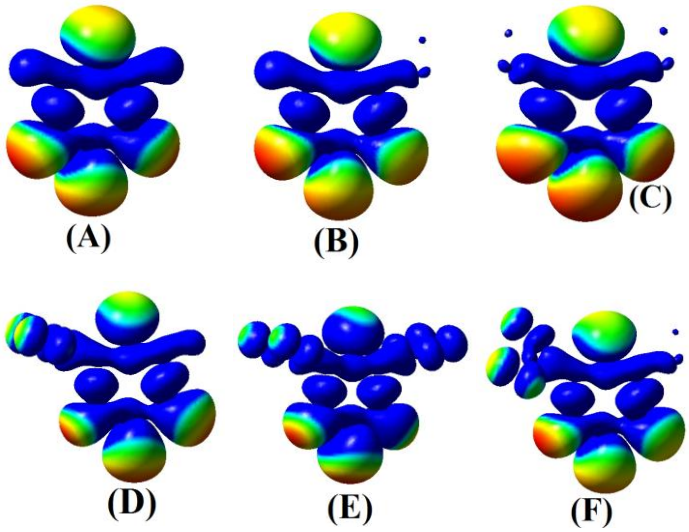

Figure 6: HOMO orbital maps of structures.

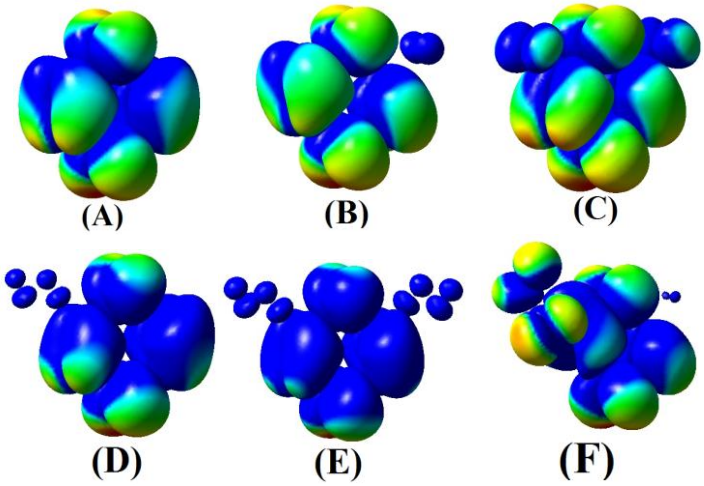

Figure 7: LUMO orbital maps of structures.

Heats of formation, predicted densities and detonation of the structures:

For the isodesmic reactions, heat of reaction ΔH at 298 K can be calculated from the following equations:

$\Delta H_{298} = \Sigma\Delta H_{f,P} - \Sigma\Delta H_{f,R}$

$\Delta H_{298.15K} = \Delta E_{298.15K} + \Delta(PV) = \Delta E_0 + \Delta ZPE + \Delta H_T + \Delta nRT$

$= \Sigma\Delta H_{f,P} - \Sigma\Delta H_{f,R}$

Where $\Delta H_{f,P}$ and $\Delta H_{f,R}$ are the heats of formation of products and reactants at 298 K, respectively. ΔE_0 and ΔZPE correspond to the total energy difference and the zero point energy difference between products and reactants at 0 K, respectively. ΔH_T is the changes in thermal correction to enthalpies between products and reactants. Δ(PV) equals ΔnRT for reaction in gas phase. For isodesmic reactions, Δn=0. As seen from the Table, the HOF order is E>D>A>F>B>C for the structures at B3LYP/6-311G(d,p) level of theory.

Furthermore, density (ρ), detonation velocity (D), and detonation pressure (P) are the important parameters to evaluate the explosive performances of high energy materials ($C_aH_bO_cN_d$) and can be predicted by the following empirical Kamlet-Jacob equations [24]:

$D=1.01(NM^{1/2}Q^{1/2})^{1/2}(1+1.3\rho)$

$P=1.558\rho^2NM^{1/2}Q^{1/2}$

Where D: detonation velocity in km/s, P: detonation pressure in GPa, ρ: density of a compound in g/cm^3, N: moles of gaseous detonation products per gram of explosive (in mol/g), M: average molecular weight of gaseous products (in g/mol), Q: chemical energy of detonation in kJ/g. Table **10** collects the predicted V, ρ, Q, D and P of the structures. As seen from the Table, the D and P order is E>C>F>D>B>A for the structures at B3LYP/6-311G(d,p) level of theory. It is noted that the D and P values gradually increase when the

substituents on the tetrazine ring are similar. In a word, it shows that the introduction of nitro group more than amino group can improve the detonation properties of the structures. For RDX and HMX, experimental value of D and P are 8.75 km/s, 9.10 km/s and 34.70 GPa, 39.00 GPa, respectively. The RDX and HMX are the current standards for detonation behavior. Comparing these values with data of Table **10** shows molecule E can be an explosive.

Stoichiometric ratio			
parameters	c≥2a+b/2	2a+b/2>c≥b/2	b/2>c
N	(b+2c+2d)/4MW	(b+2c+2d)/4MW	(b+d)/2MW
M	4MW/(b+2c+2d)	(56d+88c-8b)/(b+2c+2d)	(2b+28d+32c)/(b+d)
Q	(28.9b+94.05a+0.239ΔHf)/MW	[28.9b+94.05(c/2-b/4)+0.239ΔHf]/MW	(57.8c+0.239ΔHf)/MW

Conclusion

In this study, stabilities of six structures as potential candidates for high energy density materials (HEDMs) have been investigated computationally by using quantum chemical treatment. Full geometrical optimizations of nitrogen-rich structures were performed using ab initio and density functional theory (DFT, B3LYP) at the levels of 6-31G(d,p), 6-31+G(d,p), 6-311G(d,p), 6-311+G(d,p), cc-pvDZ. Introduction of nitro and amino groups into 1, 2, 3, 5-tetrazine compound slightly affects the BDE and HOF. The detonation performance data are calculated according to the HOFs calculated by B3LYP/6-311G(d,p) level of theory and the values of D and P increase when the number of –NO2 group increases. Also, it concluded that the all structures are viable candidate of high energy density materials (HEDMs).

Computational methods:

Computations were performed with the Gaussian 03 package [12] using the spin-restricted Hartree-Fock (RHF) and the B3LYP methods with 6-31G(d,p), 6-31+G(d,p), 6-311G(d,p), 6-311+G(d,p) and cc-pvDZ basis sets. All calculations and geometry optimization for each molecule were obtained the mentioned theories (RHF and B3LYP). The term of B3LYP consists of the Vosko, Wilk, Nusair (VWN3) local correlation functional [13] and Lee, Yang, Parr (LYP) correlation function [14, 15]. For comparing of the bond strengths, homolytic bond dissociation energy (BDE) calculations were performed by B3LYP/6-311G(d,p) level. The mentioned level was used to predict the HOFs of all molecules via isodesmic reactions. This level by gauge invariant atomic orbital (GIAO) approach was used for nucleus independent chemical shift (NICS) calculations at the center of rings. Vibrational analyses without any symmetry constraints were done for each set of calculations by the same basis set. Theoretical calculations have been performed in the gas phase [16,17]. All calculations were carried out without symmetrical restrictions. An efficient and convenient statistics average method was worked out to predict the crystalline densities of all derivatives. To calculate the densities of structures, the molecular volume data was required. The molecular volume V was defined as inside a contour of 0.001 electrons/bohr^3 density. The computational molecular density ρ (ρ=M/V, where M = molecular weight) was also calculated. Oxygen balance (OB_{100}) is an expression that is used to indicate the degree to which an explosive can be oxidized. OB_{100} was calculated as follows:

$$OB\% = \frac{-1600}{Mol.wt} \times \left(2a + \frac{b}{2} - c\right)$$

Where:

a = number of atoms of carbon, b = number of atoms of hydrogen, c = number of atoms of oxygen.

References

[1] Mahkam, M.; Nabati, M.; Latifpour, A.; Aboudi, J. *Des. Monomers Polym.* **2014,** *17,* 453.
[2] Mahkam, M.; Namazifar, Z.; Nabati, M.; Aboudi, J. *Iran. J. Org. Chem.* **2014,** *6,* 1217.
[3] Nabati, M. *Iran. J. Org. Chem.* **2015,** *7,* 1669.
[4] Nabati, M. *Iran. J. Org. Chem.* **2015,** *7,* 1631.
[5] Nabati, M.; Mahkam, M. *Org. Chem. Res.* **2016,** *1,* 156.
[6] Nabati, M. *J. Phys. Theor. Chem. IAU Iran* **2015,** *12,* 325.

[7] Nabati, M.; Mahkam, M. *J. Phys. Theor. Chem. IAU Iran* **2015,** *12,* 121.
[8] Whelan, D. J.; Spear, R. J.; Read, R. W. *Thermochim. Acta.* **1984,** *80,* 149.
[9] He, Y.; Liu, X.; Lin, M. C. *Int. J. Chem. Kinet.* **1991,** *23,* 1129.
[10] Wong, M. W. *Chem. Phys. Lett.* **1996,** *256,* 391.
[11] Nabati, M. *Iran. J. Org. Chem.* **2015,** *7,* 1577.
[12] Frisch, M. J.; Trucks, G. W.; Schlegel, H. B.; Scuseria, G. E.; Robb, M. A.; Cheeseman, J. R.; Montgomery Jr., J. A.; Vreven, T.; Kudin, K. N.; Burant, J. C.; Millam, J. M.; Iyengar, S. S.; Tomasi, J.; Barone, V.; Mennucci, B.; Cossi, M.; Scalmani, G.; Rega, N.; Petersson, G. A.; Nakatsuji, H.; Hada, M.; Ehara, M.; Toyota, K.; Fukuda, R.; Hasegawa, J.; Ishida, M.; Nakajima, T.; Honda, Y.; Kitao, O.; Nakai, H.; Klene, M.; Li, X.; Knox, J. E.; Hratchian, H. P.; Cross, J. B.; Adamo, C.; Jaramillo, J.; Gomperts, R.; Stratmann, R. E.; Yazyev, O.; Austin, A. J.; Cammi, R.; Pomelli, C.; Ochterski, J. W.; Ayala, P. Y.; Morokuma, K.; Voth, G. A.; Salvador, P.; Dannenberg, J. J.; Zakrzewski, V. G.; Dapprich, S.; Daniels, A. D.; Strain, M. C.; Farkas, O.; Malick, D. K.; Rabuck, A. D.; Raghavachari, K.; Foresman, J. B.; Ortiz, J. V.; Cui, Q.; Baboul, A. G.; Clifford, S.; Cioslowski, J.; Stefanov, B. B.; Liu, G.; Liashenko, A; Piskorz, P.; Komaromi, I.; Martin, R. L.; Fox, D. J.; Keith, T.; Al- Laham, M. A.; Peng, C. Y.; Nanayakkara, A.; Challacombe, M.; Gill, P. M. W.; Johnson, B.; Chen, W.; Wong, M. W.; Gonzalez, C.; Pople, J. A. *Gaussian 03. Revision B.01*. Gaussian Inc. Wallingford. CT. **2004**.
[13] Vosko, S. H.; Wilk, L.; Nusair, M. *Can. J. Phys.* **1980,** *58,* 1200.
[14] Lee, C.; Yang, W.; Parr, R. G. *Phys. Rev. B* **1988,** *37,* 785.
[15] Miehlich, B.; Savin, A.; Stoll, H.; Preuss, H. *Chem. Phys. Lett.* **1989,** *157,* 200.
[16] Aboudi, J.; Bayat, Y.; Abedi, Y.; Nabati, M.; Mahkam, M. *Iran. J. Chem. Chem. Eng.* **2015,** *34,* 1.
[17] Nabati, M.; Mahkam, M. *J. Phys. Theor. Chem. IAU Iran* **2015,** *12,* 33.
[18] Nabati, M.; Mahkam, M. *Iran. J. Org. Chem.* **2015,** *7,* 1419.
[19] Nabati, M.; Mahkam, M. *Iran. J. Org. Chem.* **2015,** *7,* 1463.
[20] Nabati, M.; Mahkam, M. *Iran. J. Org. Chem.* **2014,** *6,* 1397.
[21] Nabati, M.; Mahkam, M. *Iran. J. Org. Chem.* **2015,** *7,* 1503.
[22] Chung, G. S.; Schimidt, M. W.; Gordon, M. S. *J. Phys. Chem. A* **2000,** *104,* 5647.
[23] Nabati, M.; Mahkam, M. *Iran. J. Org. Chem.* **2015,** *7,* 1537.
[24] Kamlet, M. J.; Jacobs, S. J. *J. Chem. Phys.* **1968,** *48,* 23.